An improved design of fluorophilic molecules: Prediction of the ln P fluorous partition coefficient, fluorophilicity, using 3D QSAR descriptors and neural networks

ARTICLE *in* JOURNAL OF FLUORINE CHEMISTRY · MARCH 2001

Impact Factor: 1.95 · DOI: 10.1016/S0022-1139(01)00342-6

3 AUTHORS:

László E Kiss
BIAL
21 PUBLICATIONS **147** CITATIONS
SEE PROFILE

István Kövesdi
Egis Gyógyszergyár Nyrt.
40 PUBLICATIONS **470** CITATIONS
SEE PROFILE

Jozsef Rabai
Eötvös Loránd University
63 PUBLICATIONS **1,828** CITATIONS
SEE PROFILE

ELSEVIER

Journal of Fluorine Chemistry 108 (2001) 95–109

JOURNAL OF FLUORINE CHEMISTRY

www.elsevier.com/locate/jfluchem

An improved design of fluorophilic molecules: prediction of the ln *P* fluorous partition coefficient, fluorophilicity, using 3D QSAR descriptors and neural networks

László E. Kiss[a], István Kövesdi[b,1], József Rábai[a,*]

[a]*Department of Organic Chemistry, Eötvös Loránd University, P.O. Box 32, H-1518, Budapest 112, Hungary*
[b]*EGIS Pharmaceuticals Ltd., P.O. Box 100, H-1475 Budapest, Hungary*

Received 8 August 2000; accepted 9 December 2000

Abstract

A combination of 3D QSAR molecular descriptors and artificial neural networks have been used to predict fluorophilicities, the natural logarithm of the perfluoro(methylcyclohexane)/toluene partition coefficients, for a wide range of partially fluorinated organic compounds. The average error of the predictions was less than twice the 0.2 experimental error. Multiple linear regression proved to be much less efficient. To better characterise the fluorous partition phenomenon, specific fluorophilicity was defined as the product of fluorophilicity and of the ratio of the van der Waals volumes of the expelled fluorous solvent and the entering solute molecules. This dimensionless term correlates well in a compound family with the calculated Hildebrand parameters of the fluorous molecules. The trifluoromethyl group was found highly effective for increasing the fluorous phase affinities of model compounds when used in combination with longer perfluoroalkyl groups.

Keywords: Fluorine; Neural network; Fluorous partition coefficient; Specific fluorophilicity; Structure–activity relationships

1. Introduction

Organic syntheses are receiving much stimulation by the strategy-level design of both reactions and separation processes [1–9]. The recent discovery of fluorous biphase systems [1–14] and the emerging field of fluorous chemistry [15–22] provide novel means for carrying out syntheses and engineered product separations. These fluorous methods are based on the limited and temperature-controlled miscibility of the apparently non-toxic perfluorinated and standard organic or inorganic solvents and on the 'like dissolves like' principle [10]. Fluorous biphase catalysis (FBC) has a potential for industrial application [1–9], however, an acceptable partition of the catalysts toward the fluorous phase is required [8,24,25], while fluorous reactions are highly suited for liquid phase combinatorial chemistry and parallel synthesis [26–30]. These processes rely on the fine tuning of the fluorous phase affinities of the involved reagents, catalysts, reactants, or substrates by temporary or permanent attachment of fluorous phase labels. This strategy offers an easy separation for the fluorous reaction components and the other 'anti-fluorous' molecules either using fluorous/organic or aqueous liquid–liquid extraction or filtration through a fluorous reverse phase silica gel [1–30].

We propose to use the Hildebrand solubility parameter (δ) scale to locate a compound in the phasephilicity map and for the selection of immiscible phases (Scheme 1).

Perfluorinated solvents represent one extreme here with the lowest δ values, while organic solvents span a wide polarity range and the other extreme is at water with the highest value. Supercritical carbon dioxide ($scCO_2$) has a unique position due to its pressure- and temperature-dependent cohesive energy density (δ^2), which results in miscibility either with low polarity organic solvents or fluorocarbons under appropriate regimes [31]. Homogeneous, as well as biphasic systems can be selected using the phasephilicity map since solvent–solvent and solvent–solute likeness is easily estimated by the closeness of the empirical δ values [5,11,31–35].

The success of fluorous chemistry and its possible green spin-offs (Fluorous Biphase Catalysis), however, requires an

* Corresponding author. Tel.: +36-1-209-0602; fax: +36-1-209-0602.
E-mail addresses: istvan.kovesdi@matavnet.hu (I. Kövesdi), rabai@szerves.chem.elte.hu (J. Rábai).
[1] Co-corresponding author. Tel.: +36-1-265-5613; fax: +36-1-265-5613.

0022-1139/01/$ – see front matter
PII: S0022-1139(01)00342-6

δ(Fluorous solvents) <	δ(Organic solvents)	<< δ(Water /Brine)
fluorophilic	**organophilic**	**hydrophilic**
(organophobic and hydrophobic)	(hydrophobic and fluorophobic)	(organophobic and fluorophobic)
perfluorohexane(12.1)	acetonitrile(24.3)	water(48)
perfluoroheptane(12.3)	1-butanol(23.3)	ethylene glycol(34.9)
perfluorocyclohexane(12.5)	1-hexanol(22)	methanol(29.7)
perfluoro(methylcyclohexane) (12.5)	dichloromethane(19.8)	
perfluoro(tributylamine)(12.7)	chlorobenzene(19.4)	
	chloroform(19.0)	
	benzene(18.8)	
↑	toluene(18.2)	
sc-CO$_2$ (18.2 x ρ_{sc}/ρ_{liq}) →	carbon tetrachloride(17.6)	
(pressure dependent solvent power)	cyclohexane (18.8)	
CO$_2$-philic [40, 41]	benzotrifluoride(16.8)	
	hexane(14.9)	

Scheme 1. The phasephilicity map (typical solvents with their δ (MPa$^{1/2}$) values [31,33]).

effective design of highly fluorophilic molecules based on a more fundamental understanding of the structure–phasephilicity correlation [1,4–6,36–41]. In a broader sense [2,39,42] the green solvent $scCO_2$ can be regarded fluorous, as it allows the homogeneous Rh/fluorous phosphine complex catalysed hydroformylation of long chain olefins to linear aldehydes with high selectivity and reasonable rates as recently demonstrated by Koch and Leitner [43].

As a rule of thumb, the substitution of linear perfluoroalkyl chains ('fluorous ponytails' $R_{fn} = F(CF_2)_n$) of appropriate size and number for hydrogens was implemented in several laboratories for the synthesis of 'first generation' fluorophilic compounds [1–30,44–63].

Experimentally determined 'fluorophilicity' values and 'fluorous partition coefficients' revealed that there exists no simple relation between the total fluorine load and the phase preference of the molecules holding the 'fluorous ponytails' [4,44–63]. Thus, the question 'how many fluorines and what molecular structure are required to make a compound fluorous?' is still unanswered.

The solubility and partition phenomena are quite generally governed by intermolecular forces [35,41], influenced strongly by polarity. The picture is complicated for larger molecules containing different groups with different polarity and interactive characteristics. This complication can be dealt with the assumption that each group of the molecule is associated with its own unique change in chemical potential, independent of the presence of other groups, when transferred between phases [31]. Thus, compounds with high fluorous phase affinity must have an appropriate balance between their fluorous and 'anti-fluorous' (fluorophobic) domains [4,8–14,50,54]. The term 'anti-fluorous' has been introduced by Curran to specify those solvents which have poor capability to dissolve polyfluorinated molecules [56].

To quantify the extent of the fluorous phase preference for a compound '*i*', we have defined the term fluorophilicity (f_i, Eq. (1)) from the partition coefficient (P_i) between two particular solvents, perfluoro(methylcyclohexane) and toluene at 25°C temperature [50,51]. According to this definition compound '*i*' is fluorophilic if its f_i value is positive.

$$f_i = \ln P_i = \ln\left[\frac{c_i(CF_3C_6F_{11})}{c_i(CH_3C_6H_5)}\right], \quad T = 25^\circ C \tag{1}$$

In recent years the significance of careful experimental determination of fluorous partition data has been highlighted by Curran, Horváth, Gladysz, and others, thus it soon became part of the fluorous experimental protocols [63]. Since a multitude of immiscible fluorous/organic solvent pairs exist at ambient temperature the fluorous partition coefficient ($P_{i(FBS)}$) defined by Eq. (2) is much wider in scope than fluorophilicity.

$$P_i(FBS) = \frac{c_i(\text{fluorous phase})}{c_i(\text{other phase})}, \quad T = \text{ambient} \tag{2}$$

Some empirical rules, which seem to be instructive in the design of fluorophilic molecules, based on the inspection of reported fluorous partition data, structural formulae and notes on solubility behaviour are summarised below [4,8,13,26,44–63].

Rule 1: The fluorine content. At least 60 wt.% fluorine is required. Generally this composition can be achieved by appending one or more perfluoroalkyl groups, while further additions of fluorous groups can raise the fluorine content slowly to the limit defined by the composition of the ponytails themselves. However, this protocol is coupled with an intensive gain in molecular weight and cost, which could be a limiting factor for industrial FBC applications.

Rule 2: The lengths of the fluorous ponytail. Longer fluorous chains cause an increase in partition coefficient coupled with a decrease in absolute solubilities in both phases. Inversely, an increase of the share of the 'anti-fluorous' domains in the molecules concerned, results in an increase of their absolute solubilities in the organic phase [49].

Rule 3: The number of fluorous ponytails. Increasing number of the same fluorous ponytail usually results in higher partition, except [62], with acceptable absolute solubilities in the fluorous phase, when compared to the results of lengthening of a single ponytail.

Rule 4: The structure. The number of functional groups capable for intermolecular attractive interactions, via orientation forces, hydrogen bonds, or induction forces [31,35], should be kept at a minimum. This is rather important for FBC applications, where precious metal leaching and recovery issues can only be considered with the knowledge of the structure and phase behaviour of the intermediates involved in the catalytic cycle [54].

Rule 5. The structure of the fluorous ponytail. No data are available yet on the effect of branching or of hetero atoms as part of $–CF_2OCF_2–$, $–CF_2SCF_2–$, or $–CF_2N(R_f)_2$ segments, or conformational rigidity versus flexibility on the partition characteristics, when different ponytails are appended [14,23]. Similar issues, i.e. branching and flexibility of

the molecules concerned, have been addressed recently for the design and theoretical modelling of CO_2-philic compounds [40].

It is known that partition coefficients between *n*-octanol and water can be calculated with good accuracy from the chemical structures using QSAR descriptors and by other methods [64,65]. Here we investigate the prediction of fluorophilicity from calculated molecular descriptors by artificial neural networks and by multiple linear regression analysis.

2. Computational methods

The 3D structure of the molecules listed in Scheme 2 was calculated with the HyperChem program [66] using MM+ molecular mechanics and a conformational search for the global minimum conformer. During the conformational search all dihedral angles around rotatable bonds were varied and the ring flexing option was applied for the saturated rings. A minimum of 256 iterations was completed for each compound with 0.1 kcal/Å convergence criteria for the gradient. We used the obtained global minimum conformers to represent the 3D structures of the molecules in this paper. The 3D molecular structures and the fluorophilicity data were stored in MDL IsisBase format [67].

For the calculation of most 3D QSAR descriptors and for the neural network (NN) computations we used the 3DNET program [68,69]. It calculates many 2D, 3D QSAR and QSPR descriptors from MDL SDF format molecular data sets and implements MLR, PLS and NN algorithms. To begin with we selected those descriptors [70–87], listed in Table 1 that were proven to be useful in the calculation of log *P*, solubility and boiling point. We augmented this set with the fluorine content and the HOMO, LUMO energies.

Table 1
Descriptors checked for the ability to explain experimental fluorophilicity

Descriptor	Reference
Fluorine percent	cf. Table 3
Molecular mass	
Molecular volume	[70]
Molecular surface	[70]
Globularity	[71]
WHIM descriptors of mass, position, electronegativity, localised charge, atomic polarisability contribution, atomic lipophilicity contribution, atomic electro topological index	[72]
Solvent accessible surface	[70,73]
Solvent extended surface	[74]
Solvent extended volume	[74]
Calculated polarisability	[75,76]
Calculated dipole moment	[77]
Calculated lipophilicity	[78]
Calculated Hildebrand solubility parameter	[79]
Degree of chemical bond rotational freedom	[80]
Wiener index	[81]
Randic index	[82]
HDSA1, HDSA2, HASA1, HASA2 hydrogen bond descriptors	[83]
Gravitational index	[83]
Topological electronic index	[83]
QN, QO, QNO, QTOT Bodor descriptors for log *P*	[84]
Min., max. and average of ESP on the vdw surface	[75]
Histogram of ESP distribution on the vdw surface	[75]
Min., max. and average of MLP on the vdw surface	[85]
Histogram of MLP distribution on the vdw surface	[75]
Number of specified atom types	[a]
Min. max. and average of localised charge on any atom type	[75]
Electrostatic HB basicity and acidity	[86]
HOMO, LUMO (AM1)	[86]
Covalent HB basicity and acidity	[86]

[a] Investigated atom types: carbon (sp^3, sp^2, aromatic), nitrogen (sp^3, sp^2, amide, amine), oxygen (sp^3, sp^2), fluorine.

All these input descriptors used in this work are translation and rotation invariant. Since for the neural network calculations of log *P* and partition coefficients the fully connected, three-layer, feed-forward computational neural network with gradient descent training were used almost exclusively, we selected this NN model for our study. In 3DNET the gradients are calculated by back-propagation of errors [88,89] and the program uses continuously decreasing small learning rates during the learning epochs. This is not the fastest training method but always ensures convergence of the network to a global minimum when the number of input descriptors is greater than the number of hidden neurons [90]. This criterion is typical for computational chemistry applications of neural networks and was also valid in our work. The fully connected, three-layer, feed-forward neural network with bias input has found a wide range of successful applications in other areas of computational chemistry. The success stems from the mathematical property, called *universal approximation theorem*, that this type of neural networks can approximate any functions with finite number of discontinuities to arbitrary precision [91,92]. Another attractive property of this kind of neural networks is that they are *parsimonious approximators*. They give better fitting with the same number of parameters as other methods or perform equivalently or better with a smaller number of parameters [93]. In 3DNET the input and output layers of the neural networks are linear and the hidden layer neurons have tanh transfer function. Four justified mathematical criteria have been formulated for an ideal activation function and only the tanh has been found to meet all [94]. The program applies a quick and effective algorithm that calculates the relative importance of the input descriptors. This is made according to a published method [89] and similar to recent algorithms [95,96] that are used to calculate variable selection in NN calculations. It consists of adding a surplus input layer and pushing the input values towards zero in a stepwise manner. During this the back-propagation formalism tries to decrease the growing error of the calculated outcomes by restoring the effect of those inputs, by

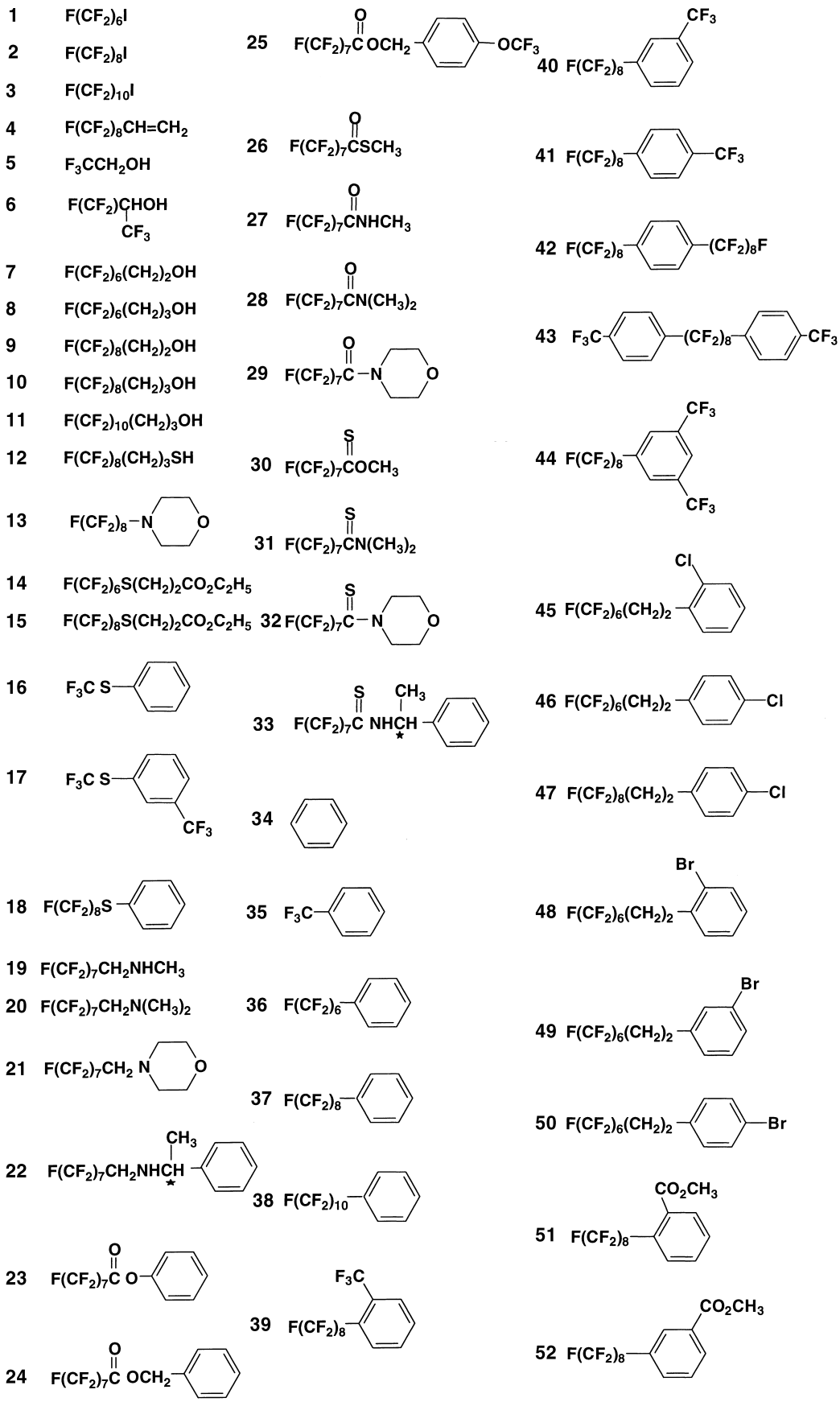

Scheme 2. Compounds submitted for neural network analysis.

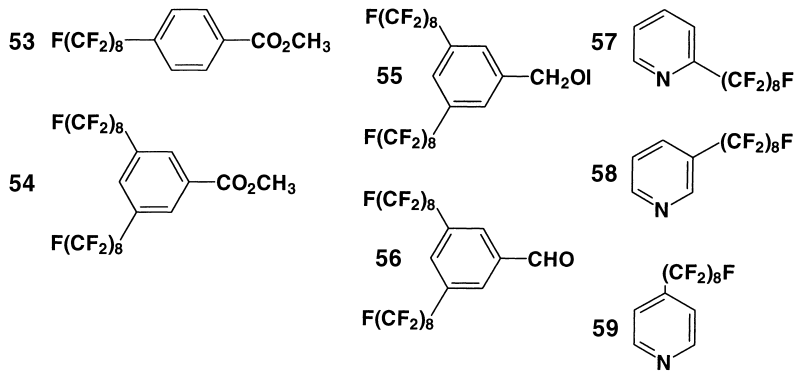

Scheme 2. (*Continued*).

increasing their connection weights, which are relevant for the calculation of the outcome. The extra network weights determined for each inputs in this way are sorted and the largest one is taken as having 100% of relative importance on a linear scale.

We searched the mathematical space of all the input descriptors listed in Table 1 to determine those that are important for the network in the reproduction of experimental fluorophilicility figures. The overtraining effect, i.e. when the converged network has worse prediction ability than at intermediate stages of convergence, is a clear sign of inadequate network architecture [88,89,97] and should be and can easily be avoided. There is no basis for believing that, having started at a random point, stopping before convergence is obtained will leave us near the best point. Since the initial weights were randomly chosen we do not know that we are approaching the optimal weights from a good direction. Even worse is that stopping training before convergence when the validation set's error bottoms out yields networks that cannot be reproduced by others. We used always at least 5 million learning epochs to practically ensure full convergence and reproducibility of our networks. In our calculations the approximation errors did not decrease noticeably after about half a million learning epochs. The 5 million epochs took less than 10 min on a Pentium III 450 MHz IBM PC. In other words the overtraining effect discarded automatically the overparametrised networks because of their poor cross-validation performance. We systematically varied the number of hidden neurons and the so-called ρ parameter. The ρ parameter is the ratio of the number of molecules and the number of network parameters. We used a bias neuron in the input layer and two, three and four hidden neurons while the ρ was scanned from 1.0 to 8.0 by changing the number of applied descriptors. We started with all of the input descriptors and with two neurons in the hidden layer. Following the convergence of the network we checked the relative importance of the input descriptors for the network. We dropped the least important descriptor and repeated the calculation with the new network. Where the ρ was above 1.0 we calculated the leave-one-out cross-validation Q^2 value for each network. These cross-validations were performed with 5 million learning epochs. We submitted those seven networks that yielded greater Q^2 figure than 0.95 to further leave-N-out cross-validations. In these more demanding validation procedures 50 randomly selected compounds consisted the training set for the networks and the remaining nine compounds were used as the test set. This leave-N-out cross-validation with 5 million learning epochs was repeated six times for all the selected networks. The finally chosen network was the most robust one against leave-N-out cross-validation. The minimum of its six leave-N-out cross-validated Q^2 values was the highest among the tested networks.

The descriptor sets of the seven best leave-one-out cross-validated networks were submitted to multiple linear regression calculations (MLR) [98]. We also repeated all the leave-one-out and leave-N-out cross-validations of the MLR models.

3. Results

The investigated compounds are listed in Table 3. Within the applied molecular mechanics approximation the perfluoroalkyl chains in the gas phase MM+ minimum energy conformers are in an anti-periplanar, zig-zag conformation.

Table 2
Descriptors effective in predicting fluorophilicity

Descriptor[a]	Relative significance of standalone inputs (%)
Solvent extended surface	100
Hildebrand solubility parameter	70
WHIM second vdw volume moment	67
WHIM third mass moment	45
WHIM first position moment	37
Degree of chemical bond rotational freedom	34
WHIM first polarisability moment	25
WHIM atomic position moment A combination	21

[a] Weighted holistic invariant molecular (WHIM) descriptors are three-dimensional molecular indexes that represent different sources of chemical information.

Table 3
Selected properties of partially fluorinated compounds

Entry	Compound[a] $R_{fn}R = F(CF_2)_nR$	F (%)	f_{exp}[b,c]	f_{pred}[d]	$\delta_{calcd}(MPa^{1/2})$[e]	$V_{vdw}(angstrom^3)$[f]	f_{spec}[g]
1	$R_{f6}I$	55.4	1.31	0.57	14.8	178.4	0.904
2	$R_{f8}I$	59.2	2.04	2.60	14.6	227.9	1.10
3	$R_{f10}I$	61.8	2.84	2.95	14.4	274.0	1.28
4	$R_{f8}CH{=}CH_2$	72.4	2.67	2.98	12.8	215.2	1.53
5	CF_3CH_2OH	57.0	−1.77	−2.08	21.6	59.6	−3.66
6	$(CF_3)_2CHOH$	67.8	−1.01	−1.08	18.4	85.9	−1.45
7	$R_{f6}(CH_2)_2OH$	67.8	0.10	0.17	17.4	187.5	0.066
8	$R_{f6}(CH_2)_3OH$	65.3	−0.23	0.01	17.4	201.5	−0.141
9	$R_{f8}(CH_2)_2OH$	69.6	1.02	0.83	16.8	156.8	0.801
10	$R_{f8}(CH_2)_3OH$	67.6	0.59	0.81	16.9	241.9	0.300
11	$R_{f10}(CH_2)_3OH$	69.0	1.42	1.21	16.4	279.2	0.626
12	$R_{f8}(CH_2)_3SH$	65.4	0.24	0.33	16.6	258.2	0.114
13	$R_{f8}N(CH_2CH_2)_2O$	63.9	0.86	0.80	14.9	251.7	0.421
14	$R_{f6}S(CH_2)_2CO_2Et$	54.6	−0.67	−0.76	16.5	260.4	−0.317
15	$R_{f8}S(CH_2)_2CO_2Et$	58.5	0.04	0.21	16.1	285.3	0.0172
16	CF_3SPh	32.0	−2.45	−1.73	18.9	103.8	−2.91
17	m-$CF_3SC_6H_4CF_3$	46.3	−1.58	−1.76	17.4	173.1	−1.12
18	$R_{f8}SPh$	61.1	0.59	0.33	16.3	271.4	0.268
19	$R_{f7}CH_2NHMe$	69.0	1.07	1.48	13.9	204.2	0.645
20	$R_{f7}CH_2NMe_2$	66.7	1.53	1.40	13.4	229.2	0.822
21	$R_{f7}CH_2N(CH_2CH_2)_2O$	60.7	0.14	0.21	15.1	265.6	0.0649
22	$R_{f7}CH_2NHCH(Me)Ph(+)$	56.6	−0.87	−0.38	16.1	289.0	−0.371
23	$R_{f7}C(O)OPh$	58.1	0.48	0.49	16.7	267.0	0.221
24	$R_{f7}C(O)OCH_2Ph$	56.5	2.14	2.23	16.8	302.8	0.870
25	p-$R_{f7}C(O)OCH_2C_6H_4OCF_3$	58.1	3.15	2.79	16.4	292.6	1.33
26	$R_{f7}C(O)SMe$	64.2	1.16	0.51	16.2	228.4	0.625
27	$R_{f7}C(O)NHMe$	66.7	0.15	0.71	16.9	223.0	0.0828
28	$R_{f7}C(O)NMe_2$	64.6	0.34	0.04	16.4	230.7	0.181
29	$R_{f7}C(O)N(CH_2CH_2)_2O$	59.0	−0.62	−0.79	18.0	269.6	−0.283
30	$R_{f7}C(S)OMe$	64.2	1.08	0.64	16.2	215.7	0.616
31	$R_{f7}C(S)NMe_2$	62.3	−0.66	−0.53	16.2	231.3	−0.351
32	$R_{f7}C(S)N(CH_2CH_2)_2O$	57.1	−1.56	−1.39	17.7	273.1	−0.703
33	$R_{f7}C(S)NHCH(Me)Ph(+)$	53.4	−1.84	−2.24	18.2	325.7	−0.695
34	C_6H_6	–	−2.76	−2.64	18.8	52.25	−6.50
35	CF_3Ph	39.0	−1.95	−2.20	16.8	81.75	−2.94
36	$R_{f6}Ph$	62.3	0.54	0.30	15.4	189.8	0.350
37	$R_{f8}Ph$	65.1	1.24	1.05	15.1	273.7	0.558
38	$R_{f10}Ph$	66.9	1.77	1.56	14.9	309.7	0.704
39	o-$R_{f8}C_6H_4CF_3$	67.4	1.50	1.09	14.6	294.6	0.627
40	m-$R_{f8}C_6H_4CF_3$	67.4	2.37	2.51	14.6	296.2	0.985
41	p-$R_{f8}C_6H_4CF_3$	67.4	2.13	2.15	14.6	310.5	0.844
42	p-$R_{f8}C_6H_4R_{f8}$	70.7	4.98	5.30	14.3	441.6	1.39
43	$[p$-$CF_3C_6H_4(CF_2)_4]_2$	60.6	−0.56	−0.71	16.2	321.0	−0.215
44	1,3,5-$R_{f8}C_6H_3(CF_3)_2$	69.1	4.07	3.97	14.3	325.0	1.54
45	o-$R_{f6}(CH_2)_2C_6H_4Cl$	53.9	−0.64	−0.87	16.5	241.1	−0.327
46	p-$R_{f6}(CH_2)_2C_6H_4Cl$	53.9	−1.02	−1.27	16.5	254.4	−0.494
47	p-$R_{f8}(CH_2)_2C_6H_4Cl$	57.8	−0.37	−1.05	16.1	293.7	−0.155
48	o-$R_{f6}(CH_2)_2C_6H_4Br$	49.1	−1.05	−0.62	16.7	259.5	−0.498
49	m-$R_{f6}(CH_2)_2C_6H_4Br$	49.1	−1.44	−1.20	16.7	269.2	−0.658
50	p-$R_{f6}(CH_2)_2C_6H_4Br$	49.1	−1.49	−1.27	16.7	252.4	−0.727
51	o-$R_{f8}C_6H_4CO_2Me$	58.3	−0.39	−0.36	16.6	274.4	−0.175
52	m-$R_{f8}C_6H_4CO_2Me$	58.3	0.12	−0.11	16.6	263.0	0.0561
53	p-$R_{f8}C_6H_4CO_2Me$	58.3	−0.01	0.60	16.6	318.0	−0.00387
54	1,3,5-$(R_{f8})_2C_6H_3CO_2Me$	66.4	4.45	4.43	15.3	493.0	1.11
55	1,3,5-$(R_{f8})_2C_6H_3CH_2OH$	68.4	3.64	3.96	16.5	463.4	0.967
56	1,3,5-$(R_{f8})_2C_6H_3CHO$	68.6	4.29	4.20	15.7	422.5	1.250
57	2-$R_{f8}C_5H_4N$ (pyridine)	65.0	0.54	0.64	16.1	235.6	0.282
58	3-$R_{f8}C_5H_4N$ (pyridine)	65.0	0.88	0.87	16.1	231.7	0.468
59	4-$R_{f8}C_5H_4N$ (pyridine)	65.0	0.80	0.96	16.1	249.7	0.394

[a] Compound's source, see Section 5.
[b] Determined in this study; however, for compounds **2**, **5–11**, **13**, **15**, **20–22**, **26**, and **30–33** we used our published data [50,51].
[c] Average of three measurements with a standard deviation of about 0.2.
[d] Leave-one-out cross-validation results of the proposed network model, see Table 2.
[e] Hildebrand parameters from group contribution values [79].
[f] Molecular volumes were calculated according to Bodor et al. [87].
[g] Defined in Eq. (7).

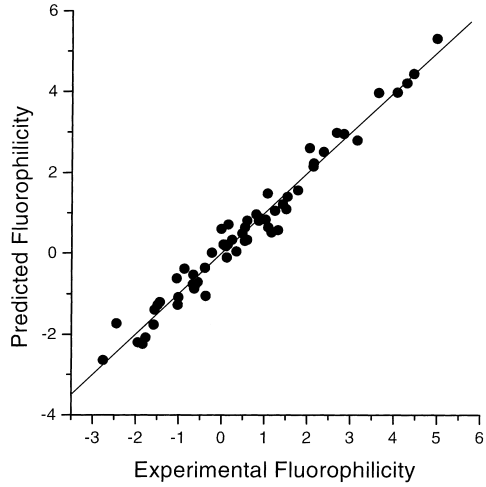

Fig. 1. Predicted vs. experimental fluorophilicity.

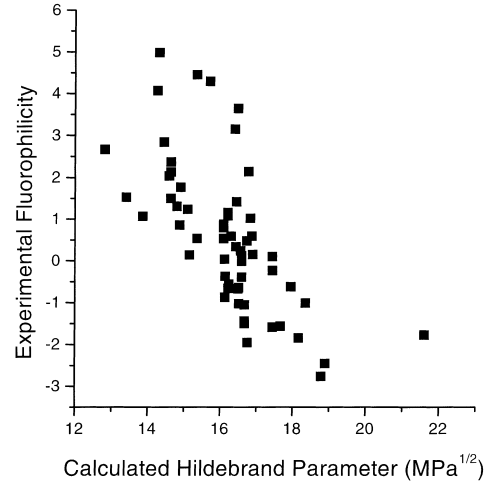

Fig. 3. Experimental fluorophilicity vs. calculated Hildebrand parameter.

Only the α and β CF_2 groups next to the organic domain are more or less distorted from this spatial arrangement. If there are two perfluoroalkyl chains in the same molecule these chains are in close contact or almost parallel position.

A large pool of calculated QSAR descriptors (Table 1) were systematically searched to find those that yield the best fluorophilicity predictions. Performances of the obtained networks were evaluated using cross-validations. The finally selected NN model contains three hidden neurons and eight input descriptors, with a ρ parameter of 1.97. We list its descriptors (Table 2) along with their relative importance for the network to reproduce fluorophilicity data.

This NN gave a 0.97 Q^2 value for the leave-one-out cross-validation and its worst leave-N-out Q^2 figure was 0.82 among six random trials. The standard error of the leave-one-out cross-validation was 0.31, which is less than twice the 0.2 experimental error of the fluorophilicity measurements (Fig. 1).

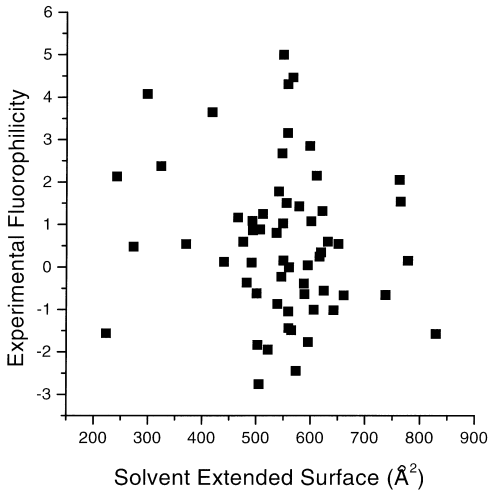

Fig. 2. Experimental fluorophilicity vs. solvent extended surface.

The seven best descriptor set containing 6–12 descriptors for the neural networks were analysed using multiple linear regression fitting of the experimental fluorophilicity figures. The leave-one-out cross-validation of the obtained MLR equations gave inferior results as compared with those of the NN calculations. The highest leave-one-out Q^2 value was 0.37 for the MLR models. Performing the same leave-N-out cross-validations, the highest minimum of the obtained Q^2 values from six random test results among the seven MLR models was only 0.18. This shows the non-linear effect of the parameters in the calculation of fluorophilicity and justifies the application of the inherently non-linear NN methodology. The non-linear correlations of the two most important descriptors, namely solvent extended surface (Table 2) and Hildebrand parameter (Table 3) with experimental fluorophilicity are displayed in Figs. 2 and 3.

4. Discussion

Neither the percentage of fluorine content nor the number of fluorine atoms in the molecule proved to be important for calculation of fluorophilicity for the set of compounds (**1**–**59**). This is probably because the fluorine content of the molecules in this study generally is high and does not show very large variation. It is between 49 and 69% with the exception of benzene.

The network instead focused on the spatial distribution of atoms and atomic properties since five of the descriptors in the final model are so called WHIM descriptors that represent different sources of chemical information. These particular five descriptors emerged from the 49 WHIM descriptors calculated by 3DNET during the network optimisation process. WHIM descriptors contain information about the whole of 3D molecular structure in terms of size, shape, symmetry and atom distribution. These indexes are

calculated from the Cartesian coordinates of the atoms weighted in different manners and represent a very general approach to describe molecules in a unitary conceptual framework.

The fluorous parts of the molecule are usually on the outer regions and, therefore, the relatively heavy fluorine atoms strongly influence the moment of inertia ellipsoid of the molecule. This is in agreement with the significance of the WHIM third mass moment in this NN. Furthermore, rod-like molecules are recognised with NN by the first moments, which are high for long perfluoroalkylated compounds. Fluorine content itself, however, is mandatory for fluorophilicity, but the magnitude of this value can be improved by the appropriate distribution of fluorine atoms. Although the weakness of Rule 1 can also be seen from experimentally determined fluorophilicity values, when a larger pool of those is concerned (Fig. 4), the requirement of $\%F > 60$ for fluorophilic molecules ($f > 0$, Eq. (1)) is a good starting point.

The final NN model uses the Hildebrand parameter (δ). This parameter describes the cohesive energy density ($c = \delta^2$) of the substances and correlates strongly with polarity of the molecules. For so called regular solutions, where small solute molecules disperse randomly among like-size solvent molecules and both solute and solvent molecules interact via London dispersion forces only, the $\ln(P_{\alpha\rightarrow\beta})$ of the 'i' solute molecules between solvents α and β can be approximated as (Eq. (3)).

$$\ln P_{\alpha\rightarrow\beta} = \left(-\frac{V_i}{RT}\right)(\delta_\beta - \delta_\alpha)(\delta_\beta + \delta_\alpha - 2\delta_i) \tag{3}$$

where V_i is the molar volume of the solute 'i', δ_i, δ_α and δ_β are, respectively, the Hildebrand parameters of solute 'i' and solvents α and β [31]. Since the solvent cohesive interactions decrease from water to non-aqueous polar protic solvents, to dipolar aprotic solvents, to apolar solvents, and finally to perfluorinated solvents (Scheme 1), the same sequence is expected for the magnitude of partition coefficients of a probe molecule 'i' measured with different fluorous (β)-organic (α) pairs (Eq. (3)).

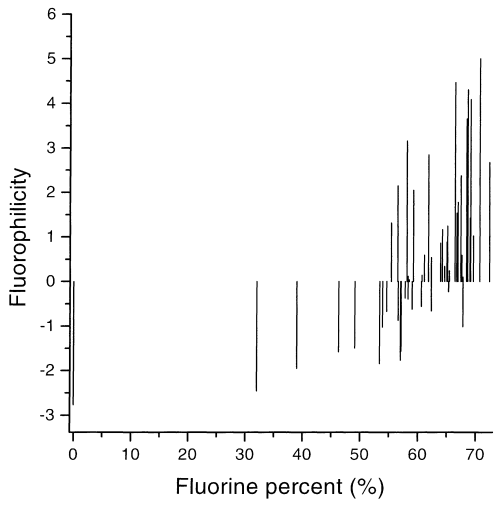

Fig. 4. Plot of fluorophilicity vs. fluorine percentage.

Theoretically the Hildebrand parameter should be among the descriptors explaining partitions between solvents and after a systematic descriptor evaluation procedure it is there. The solvent–solute interactions determine the partition equilibrium, a $\log P$ partition coefficient can be modelled by linear solvation energy relationship (LSER) with the following terms (Eq. (4)) [36,37]

$$\log P = \text{cavity} + \text{polarisability(dipolarity)} + \text{hydrogen bonding} + \text{intercept} \tag{4}$$

Solvation of the fluorous solute molecules is enthalpically unfavourable if the solvent molecules have strong cohesive interactions. High cohesive interactions make it more favourable for solvent molecules to interact with each other than with the solute molecules. The cohesive pressure c (MPa) measures the total molecular cohesion per unit volume of solvent and is defined by Eq. (5), where ΔU_{vap} and ΔH_{vap} are, respectively, the energy and enthalpy (heat) of vapourisation of the solvent to a gas of zero pressure and V_{m} is the molar volume of the solvent [38].

$$c = \frac{\Delta U_{\text{vap}}}{V_{\text{m}}} = \frac{\Delta H_{\text{vap}} - RT}{V_{\text{m}}} \tag{5}$$

$$\delta = c^{1/2} \tag{6}$$

Upon evaporation of a solvent to a non-interacting vapour, all intermolecular interactions will be broken. Cohesive pressure is related to the energy required to create cavities in a liquid in order to accommodate solute molecules, e.g. fluorous molecules, during the process of dissolution. Such cavities are also created when solute molecules are partitioning between two immiscible solvents. In comparing solvents, those which have larger c values exhibit greater cohesive interactions, and therefore, cavity formation is less favourable. The solubility parameter δ ($\text{MPa}^{1/2}$) by Hildebrand and Scott is defined as the square root of the cohesive pressure c of solvents (Eq. (5)) [34].

Specific fluorophilicity, $f_{\text{spec}}(i)$, has been defined by us [99] for compound 'i' by Eq. (7), where the ratio of the van der Waals volumes of the expelled fluorous solvent, $V_{\text{vdw}}(CF_3C_6F_{11})$, and of the entering solute molecules, $V_{\text{vdw}}(i)$, compensates for the cavity formation energy differences in both phases caused by size and keeps this novel term dimensionless.

$$f_{\text{spec}}(i) = \frac{f(i)V_{\text{vdw}}(CF_3C_6F_{11})}{V_{\text{vdw}}(i)} \tag{7}$$

The correlation of specific fluorophilicity with calculated Hildebrand parameter for compounds **1–59** is displayed in Fig. 5. The Hildebrand parameters here were obtained using a group contribution method [79], however, an update and improvement of the latter database is required for the treatment of more complex fluorine containing molecules

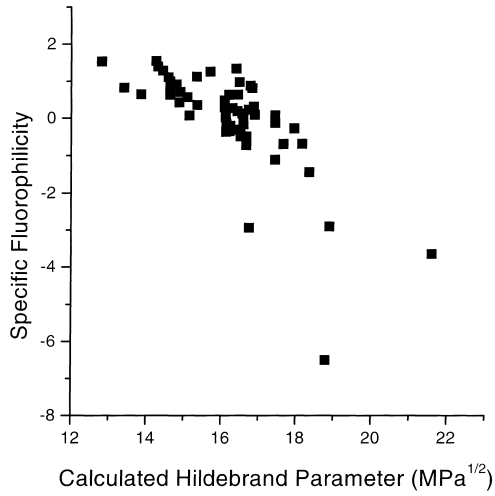

Fig. 5. Specific fluorophilicity vs. calculated Hildebrand parameter.

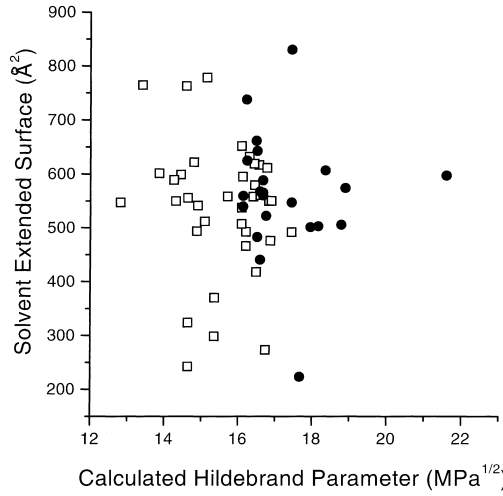

Fig. 6. Display of fluorophilic (□) and organophilic (●) compounds as a function of calculated Hildebrand parameter and solvent extended surface: a two-dimensional phasephilicity map.

than used in this study. This parameter (δ) can also be calculated from reported boiling points and densities with Hildebrand's empirical equation [32]. Obviously, the correlation of specific fluorophilicity data with δ (Table 6) is not as good as that of fluorophilicity and top eight descriptors (Table 3), since solvent cohesive interactions represent only one of the major solvent properties that reflect solvation effects.

The solvent extended surface is in strong correlation with the molecular volume and has also been proved to be important to explain log P data of alkenes [100]. The degree of rotational freedom around chemical bonds is an entropy-like descriptor in the classical QSAR studies [78], but here may only covary with other significant factors, although the covariance in the final descriptor set is low.

The two most important descriptors, the solvent extended surface and the calculated Hildebrand parameter (Table 2), can be used to create a 2D phasephilicity map (Fig. 6). It is important to note, that only the Hildebrand parameter biases the investigated compounds into fluorophilic and organophilic ones. Any changes in the solvent extended surface do not separate these compounds according their phase preference. Thus, for practical reasons, we will use only Hildebrand parameter for a rough estimation of fluorophilicities.

We propose here a bench-top 2D approach for quick estimation of specific fluorophilicity using a simple group contribution method for calculating Hildebrand parameters and molar volumes of target molecules. To show that this could become a first approximation for predicting fluorophilicities, we analysed appropriate data taken from this study and the literature (Tables 3–5). As is displayed in Figs. 7–10, a linear relation was found between specific fluorophilicity and the calculated Hildebrand parameter of the target molecules. The parameters of regression equation (Eq. (8)) are shown in Table 6, where R, S.D. and N are the measure of fitting, standard deviation, and the number of examples, respectively.

$$f_{\text{spec}} = A + B\delta \tag{8}$$

Table 4
Partition of some fluorous phosphines[a]

Entry	Compound	ln P_{FBS}	δ_{calcd} (MP$^{1/2}$a)[b]	V_{m} (cm^3 mol^{-1})[b]	f_{spec}[c]
60	ClRh[P($CH_2CH_2R_{f6}$)$_3$]$_3$	6.56	–	~1840	<0.69
61	HRh(CO)[P($CH_2CH_2R_{f6}$)$_3$]$_3$	5.25	–	~1860	<0.55
62	ClRh[P($CH_2CH_2R_{f8}$)$_3$]$_3$	6.72	–	~2250	<0.59
63	P($CH_2CH_2R_{f6}$)$_3$	4.41	13.75	613	1.41
64	O=P($CH_2CH_2R_{f6}$)$_3$[d]	>5.81	–	~620	>1.84
65	P($CH_2CH_2R_{f8}$)$_3$	>5.81	13.73	751	>1.52
66	P($CH_2CH_2CH_2R_{f8}$)$_3$	4.41	13.99	799	1.08
67	P($CH_2CH_2CH_2CH_2R_{f8}$)$_3$	4.50	14.21	847	1.04
68	(menthyl)P($CH_2CH_2R_{f6}$)$_2$	1.29	14.77	569	0.44
69	(menthyl)P($CH_2CH_2R_{f8}$)$_2$	2.70	14.61	661	0.80

[a] Measured at 27°C [53,54].
[b] Calculated from group increments [79].
[c] $f_{\text{spec}} = (V_{CF_3C_6F_{11}}/V_{\text{m}}) \ln P_{\text{FBS}}$, where $V_{CF_3C_6F_{11}} = 196\ \text{cm}^3\ \text{mol}^{-1}$.
[d] For [O=P($CH_2CH_2R_{f6}$)$_3$]$_2$, the volume is $2V_{64}$, thus $f_{spec} > 0.92$.

Table 5
Partition data of some fluorous tin hydrides[a]

Entry	Compound	ln P_1	(V_{FC72}/V_m) ln P_1	ln P_2	(V_{FC72}/V_m) ln P_2	δ_{calcd}(MPa$^{1/2}$)[b]	V_m(cm^3 mol^{-1})[b]
70	$(R_{f4}CH_2CH_2)_3SnH$	1.76	0.76	2.35	1.02	13.89	478
71	$(R_{f6}CH_2CH_2)_3SnH$	5.08	1.71	3.81	1.28	13.74	616
72	$(R_{f4}CH_2CH_2CH_2)_3SnH$	0.83	0.33	0.18	0.071	14.26	526
73	$(R_{f6}CH_2CH_2CH_2)_3SnH$	1.86	0.58	2.30	0.72	14.13	664
74	$(R_{f6}CH_2CH_2)Sn(CH_3)_2H$	0.88	0.67	−0.36	−0.27	14.36	273
75	$(R_{f8}CH_2CH_2)Sn(CH_3)_2H$	2.64	1.71	0.92	0.60	14.24	319
76	$(R_{f10}CH_2CH_2)Sn(CH_3)_2H$	3.87	2.19	1.55	0.88	14.17	365

[a] P_1 and P_2 partition coefficients are for FC72-CH_3CN and FC72-C_6H_6 systems, respectively [56].
[b] Calculated from group increments; for FC72 (perfluorohexanes) $V_{FC72} = 207$ cm^3 mol^{-1} was obtained [79].

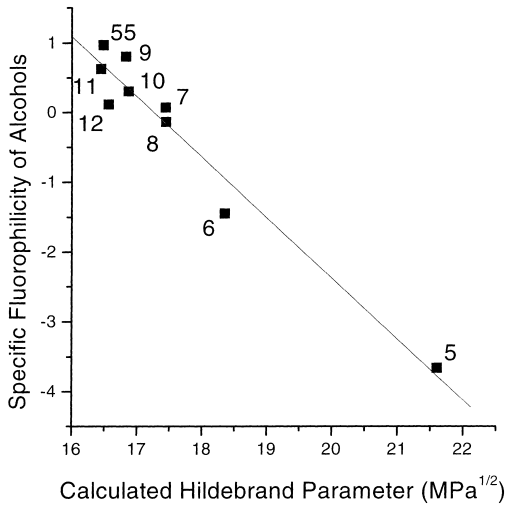

Fig. 7. Specific fluorophilicity vs. calculated Hildebrand parameter for alcohols.

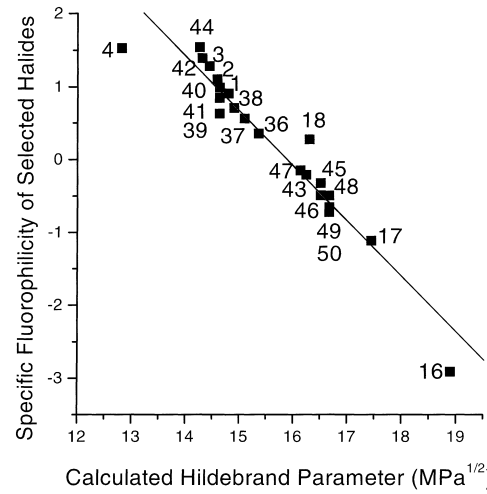

Fig. 9. Specific fluorophilicity vs. calculated Hildebrand parameter for selected halides.

It can be seen, that within different compound families, such as alcohols, organic halides, phosphines, and tin hydrides, the specific fluorophilicity correlates well with the calculated Hildebrand parameter.

Thus, a simple protocol would involve the careful experimental determination of the partition coefficients for some probe molecules, followed by the calculation of a regression equation, and finally the optimisation stage. Since the

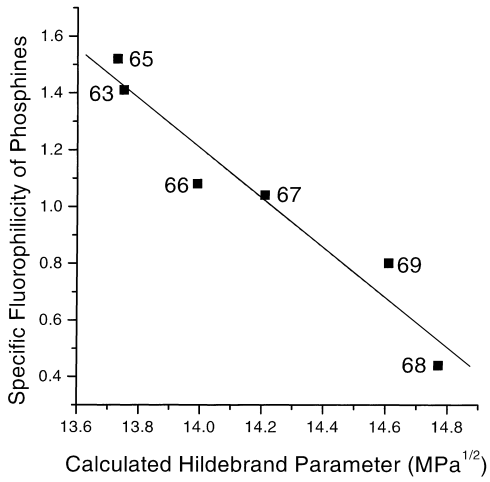

Fig. 8. Specific fluorophilicity vs. calculated Hildebrand parameter for selected phosphines.

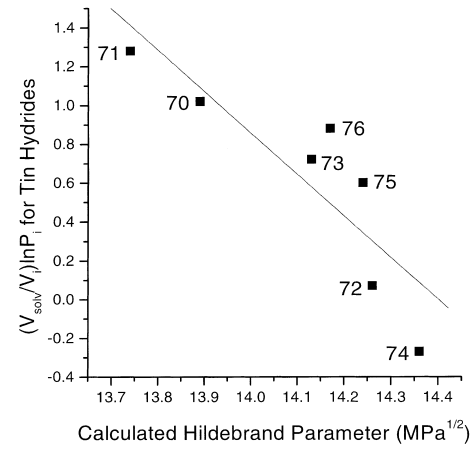

Fig. 10. Specific fluorophilicity vs. calculated Hildebrand parameter for tin hydrides.

Table 6
Regression parameters of some compound families[a]

Family	*A*	*B*	*R*	S.D.	*N*
Alcohols (Fig. 7)	14.99	−0.869	−0.975	0.344	9
Phosphines (Fig. 8)	13.48	−0.877	−0.968	0.111	6
Halides (Fig. 9)	11.98	−0.755	−0.962	0.294	22
All (**1**–**59**) (Fig. 5)	10.86	−0.67	−0.725	0.924	59
Tin hydrides (Fig. 10)	30.76	−2.14	−0.867	0.296	7

[a] For estimation of specific fluorophilicity, see Eq. (8), Tables 3 and 5.

Hildebrand parameter and molecular volume of target molecules are easily calculated from group contributions, the effect of lengths, number and shape (e.g. branching (Table 7)) of the fluorous ponytails and the molecular structure on the magnitude of the partition coefficient is predictable via Eqs. (7) and (8). Some simple calculations show, that Rules 2–5 can be interpreted in terms of Hildebrand parameters and molar volumes.

Thus, any structural changes which lead in general to the decrease of the Hildebrand parameter (e.g. removal of functional groups capable of hydrogen-bonding, decrease of polarisability, or appending $Si(CH_3)_3$ groups [58,59]) of the molecules considered and simultaneously which results higher molecular volumes are expected to increase the fluorous partition coefficients. To address the effect of volume upon partition, one can predict by Eq. (7), that dimer formation would result in an increase of the original partition coefficient (P) to the power of 2 (P^2). Molecular association could be the reason for the surprising fact, that the more polar phosphine oxide (**64**) of Gladysz et al. has higher fluorous partition coefficient than its precursor phosphine (**63**). The very high values for tris(phosphino)rhodium complexes compared to their precursors, such as $P_{60} = 713$ versus $P_{63} = 82$, and $P_{62} = 832$ versus $P_{65} = 332$ (Table 4), can be related to the increase in molecular volume during complex formation [53,54]. Similar observations were published very recently by Deelman et al. on the fluorous phase affinities of perfluoroalkylalkylsilanyl substituted triaryl phosphines (e.g. $[p\text{-}(R_{fn}CH_2CH_2)_xSi(CH_3)_yC_6H_4]_3P$, where $x + y = 3$) [62]. An inspection of the experimental fluorophilicity data listed in Table 3 also proves that this approach is viable for the design of fluorophilic compounds. However, it is important to note that trifluoromethyl groups, either introduced as such, or part of OCF_3 and SCF_3 groups, are highly effective in the increase of fluorophilicities. Thus, a trifluoromethyl group could be regarded as a 'superdense' fluorophilic group due to its high fluorine content and low formula weight coupled with small cohesion increments. Furthermore, the correlation equation between specific fluorophilicity and Hildebrand parameter could be regarded as a partition isotherm (Eq. (8)), since their parameters are related to pressure (δ, $MPa^{1/2}$) and volume ($f_{spec} = (V_{CF_3C_6F_{11}}/V_{vdw}) \ln P$).

Table 7
Estimation of the effect of branching on Hildebrand parameter

	$^z\Delta U$ (kJ mol^{-1})[a]	$^z\Delta U$ (cm^3 mol^{-1})[a]
$CF_3(CF_2)_7C_6H_5$ (**37**)[b]		
$1CF_3$	1 × 4.27	1 × 57.5
$7CF_2$	7 × 4.27	7 × 23.0
$1C_6H_5$	1 × 31.9	1 × 71.4
$^z\sum$	66.06	289.9
$(CF_3)_3CCF_2(CF_3)_2CC_6H_5$ (*i*-**37**)[c]		
$5CF_3$	5 × 4.27	5 × 57.5
$1CF_2$	1 × 4.27	1 × 23.0
$2C(-)_4$	2 × 1.47	2 × (−19.2)
$1C_6H_5$	1 × 31.9	1 × 71.4
$^z\sum$	60.46	343.5

[a] Group contribution to the molar vapourisation energy and molar volumes at 25°C [79].
[b] $\delta = (66{,}060/289.9)^{1/2} = 15.1\ MPa^{1/2}$.
[c] $\delta = (66{,}460/343.5)^{1/2} = 13.3\ MPa^{1/2}$.

An extrapolation of the partition isotherm to the lowest δ values (e.g. $\delta_{(CF_3C_6F_{11})} = 12.5\ MPa^{1/2}$) suggests that there exists a limiting value for specific fluorophilicity, which could be approximated with the virtual fluorophilicity of perfluoro(methylcyclohexane) (PMCH). This value, $f_{PMCH} = 4.1$, was obtained from the reported composition data of the equilibrated PMCH/toluene solvent pair [54].

To answer the question, how fluorous is a compound '*i*', we define a novel term, thermodynamic *fluorousness*, by Eq. (9). Here the ratio of specific fluorophilicities of compound '*i*', $f_{spec}(i)$, designated for fluorous application, and of PMCH, a representative fluorous solvent, is a fundamental measure of their likeness, when partition equilibria are concerned.

$$\%f_{ness}(i) = \frac{100 f_{spec}(i)}{f_{spec}(\mathrm{PMCH})} = 24.4 f_{spec}(i) \quad (9)$$

The identification of higher generation fluorophilic groups and the development of convenient methods for their introduction, resulting in a greater increase of fluorousness, when compared to linear perfluoroalkyl groups are in progress. These results will be published elsewhere.

5. Experimental details

5.1. Computation

Molecular volumes (V_{vdw}, Table 3) were calculated according to Bodor et al. [87]. Numerical values for atomic radii (angstrom) in these calculations are: H 1.08; C 1.53; N 1.40; O 1.36; F 1.29; Cl 1.60; Br 1.80; I 2.05; S 1.70; P 1.75; Si 2.10. We obtained $V_{vdw}(CF_3C_6F_{11}) = 123.1\ Å^3$ for perfluoro(methylcyclohexane).

5.2. Chemistry

Most of the compounds used in this study are either commercially available (**1**–**10**, **16**, **34**, **35**, **36** (ABCR, Apollo, Fluorochem)) or can be prepared according to

literature examples (**11** [51], **12** [101], **13–15** [50], **17** [102], **18** [103], **19–22** [50], **24** [104], **26** [50], **27** [105], **28–33** [50], **37** [106], **38** [107], **42** [108], **39–44** (cf. [106]), **45–50** [22,109,110], **51** [111], **52**, **53** [112], **54** [113], **57–59** [114–116]). We thank Prof. W. Leitner for samples of (*F*-alkylethyl)chloro- and bromobenzenes (**45–50**). The other reagents were purchased from Aldrich, Fluka and Merck. The structures of all new compounds (**14**, **19**, **23**, **25**, **39**, **40**, **41**, **43**, **44**, **55**, **56**) were confirmed by FT-IR (Bruker IFS 55), ^{1}H, and ^{19}F NMR spectroscopy (Varian INOVA 400, 400 MHz for ^{1}H) using TMS and $CFCl_3$ as internal standards in a solvent mixture of 1:1 (v/v) $CDCl_3$ and freon-113 ($CF_2ClCFCl_2$). Mass spectra were determined on a VG ZAB2-SEQ tandem mass spectrometer using electron impact (70 eV) for ionisation and direct probe for sample introduction at a source temperature of 180–250°C. Mass range (*m/z*) from 25 to 1500 was considered. Microanalyses were performed at our Department of Chemistry (Dr. H. Medzihradszky-Schweiger) and found in agreement with calculated values. Fluorophilicities were determined by GC analysis of the equilibrated (25°C) toluene and perfluoro(-methylcyclohexane) phases as reported earlier by us using samples of purity higher than 98% (Hewlett-Packard 5890 Series II, PONA (cross-linked methylsilicone gum) $50\,m \times 0.2\,mm \times 0.5$ μm column, H_2 carrier gas, FID detection) [51,60].

5.3. Ethyl (3-perfluorohexylthio)propionate (*14*)

Perfluorohexyl iodide (18.73 g, 42 mmol) and ethyl 3-mercaptopropionate (5.37 g, 40 mmol) in liquid ammonia (200 ml) was UV-irradiated and refluxed using a Tungsram HGL 125 lamp. Evaporation of ammonia left a solid residue, which was dissolved in ether (150 ml), washed with brine ($2\,ml \times 50$), and dried ($MgSO_4$). Short path distillation (bath temperature 100–110°C/16 mmHg) gave 14.3 g (79%) product as a pale yellow oil. GC*:* 99%, FT-IR: (liquid film), *v* (cm^{-1}): 2988.5 (CH), 1737.1 (C=O), ^{1}H NMR (δ, ppm): S–CH_2 3.19, –CO–CH_2 2.74, O–CH_2 4.19, CH_3 1.28, ^{19}F NMR (δ, ppm): CF_3 −81.4, S–CF_2 −88.1. *Elemental analysis*. Calcd. (%) for $C_{11}H_9F_{13}O_2S$ (452.2): C 29.22, H 2.01, F 54.61, S 7.09; found: C 29.1, H 2.3, F 54.3, S 7.3.

5.4. N-methyl-1H,1H-perfluorooctyl amine-1 (*19*)

Under an argon atmosphere to a solution of amide **27** (20 g, 42 mmol) and sodium borohydride (7.85 g, 208 mmol) in diethylene glycol dimethyl ether (150 ml) boron trifluoride etherate (49 g, 34.5 mmol) at room temperature was added. The mixture was then refluxed for 3 h. It was carefully acidified with 1 N HCl to $pH = 1$, the precipitate formed (amine hydrochloride) was filtered and thoroughly washed with 1 N HCl and water (each 100 ml). This solid was then treated with 0.1 N $NaHCO_3$ solution (100 ml) and extracted with ether ($3\,ml \times 40$). The organic phase was dried ($MgSO_4$) and fractionated at reduced pressure to yield 15.6 g (74%) colourless oil of bp: 56°C/16 mmHg. GC*:* 99%, FT-IR: (liquid film), *v* (cm^{-1}): 2951.3, 2866.7, 2821.1 (CH), 1254, 1207.9 (CF), ^{1}H NMR (δ, ppm): CH_3 2.57, CH_2 3.23, ^{19}F NMR (δ, ppm): CF_3 −81.5, CH_2–CF_2 −118.4. *Elemental analysis*. Calcd. (%) for $C_9H_6F_{15}N$ (413.1): C 26.17, H 1.46, F 68.98; found: C 26.0, H 1.7, F 68.7.

5.5. Phenyl perfluorooctanoate (*23*)

To a suspension of sodium hydride (0.36 g, 15 mmol) in ether (40 ml) phenol (0.94 g, 10 mmol) with stirring was added (**Caution**! H_2 evolution). When the hydrogen evolution ceased, the excess of sodium hydride was removed by filtration under an argon atmosphere. After addition of triethylamine (2.02 g, 20 mmol) and perfluorooctanoyl chloride (4.32 g, 10 mmol) the mixture was refluxed for 2 h, then the solvent was evaporated at reduced pressure (Rotavap). The residue was suspended in petroleum ether (20 ml) and transferred to a short chromatography column (SiO_2, Merck 60). The appropriate fractions (R_F: 0.4) were combined and evaporated to yield a colourless oil, 2.89 g (59%). GC: 99%, FT-IR: (liquid film), *v* (cm^{-1}): 3069.3, 3049.6, 2932.3 (CH), 1795.8 (C=O). ^{1}H NMR (δ, ppm): H (Ar, 2.5) 7.23, H (Ar, 3.5) 7.47, H (Ar, 4) 7.36, ^{19}F NMR (δ, ppm): CF_3 −81.5, (CO)–CF_2 −118.6. *Elemental analysis*. Calcd. (%) for $C_{14}H_5F_{15}O_2$ (490.2): C 34.31, H 1.03, F 58.14; found: C 34.1, H 1.4, F 57.8.

5.6. 4-(Trifluoromethoxy)benzyl perfluorooctanoate (*25*)

To a stirred soluion of 4-trifluoromethoxy-benzyl alcohol, triethyl amine (0.69 ml, 5 mmol) in dichloromethane at 20°C a solution of perfluorooctanoyl chloride (2.16 g, 5 mmol) in dichloromethane (10 ml) was added for 15 min. The mixture was stirred at room temperature for 2 h. It was washed with 1 N potassium hydrogen carbonate solution and water. After drying (Na_2SO_4), the solvent was evaporated and the product isolated by short path distillation at 16 mmHg, bp: 135–145°C (bath temperature). Yield: 1.50 g (51%) colourless oil. GC: 98.6%, FT-IR: (liquid film), *v* (cm^{-1}): 1783.7 (C=O), ^{1}H NMR (δ, ppm): CH_2 5.37, H (Ar, *o*-OCF_3) 7.24, H (Ar, *m*-OCF_3) 7.42, ^{19}F NMR (δ, ppm): OCF_3 −58.6, CF_2CF_3 −81.4, (CO)CF_2 −118.8. *Elemental analysis*. Calcd. (%) for $C_{16}H_6F_{18}O_3$ (588.2): C 32.67, H 1.03, F 58.14; found: C 32.3, H 1.3, F 57.9.

5.7. General procedure for the synthesis of compounds *39, 40, 41, 43, 44*.

Under an argon atmosphere a mixture of copper bronze (3.5 g, 55 mmol) and perfluorooctyl iodide (6.0 g, 11 mmol) or 1,8-diiodoperfluorooctane (3.6 g, 5.5 mmol) in dimethyl sulfoxide (20 ml) was stirred at 120°C for 1 h. At this point to the stirred mixture the appropriate aryl iodide (10 mmol) was added and it was kept at 130–135°C for 6 h (but 20 h for

41). The reaction mixture was poured into saturated aqueous potassium iodide solution (50 ml), then extracted with ether ($3\,ml \times 30$). The ether solution was dried ($MgSO_4$) and the solvent evaporated. The product obtained was purified by short path distillation or crystallisation.

5.8. 2-Perfluorooctyl benzotrifluoride (**39**)

Yield: 2.71 g (48%) colourless oil, bp: 135–145°C (bath temperature) at 16 mmHg. GC: 98%, ^{1}H NMR (δ, ppm): H (Ar) 7.6–7.8 m, ^{19}F NMR (δ, ppm): CF_2CF_3 −81.4, Ar–CF_2 −105.2, Ar–CF_3 −58.9, MS (*m/z*): 564 (<0.1%)M^+, 545 (2%) $(M - F)^+$, 195 (100%) $(M - C_7F_{15})^+$, 69 (18%) (CF_3). *Elemental analysis*. Calcd. (%) for $C_{15}H_4F_{20}$ (564.2): F 67.35; found: F 67.2.

5.9. 3-Perfluorooctyl benzotrifluoride (**40**)

Yield: 3.68 g (65%) colourless oil, bp: 110–120°C (bath temperature) at 16 mmHg. GC: 99.5%, ^{1}H NMR (δ, ppm): H (Ar, *m*-CF_3) 7.65, H (Ar, *p*-CF_3) 7.79, H (Ar, *p*-CF_2) 7.85, H (Ar, *o*-CF_3, *o*-CF_2) 7.86, ^{19}F NMR (δ, ppm): Ar–CF_3, −63.7, CF_2CF_3 −81.5, Ar–CF_2 −111.5, MS (*m/z*): 564 (<0.1%) M^+, 545 (3%) $(M - F)^+$, 195 (100%) $(M - C_7F_{15})^+$, 69 (15%) (CF_3). *Elemental analysis*. Calcd. (%) for $C_{15}H_4F_{20}$ (564.2): F 67.35; found F 67.1.

5.10. 4-Perfluorooctyl benzotrifluoride (**41**)

Yield: 4.58 g (81%) colourless oil, bp: 125–130°C (bath temperature) at 16 mmHg, solidifies at room temperature, mp: 41–42°C. GC: 99.8%, ^{1}H NMR (δ, ppm): H (Ar, *o*-CF_3) 7.72, H (Ar, *o*-CF_2) 7.77, ^{19}F NMR (δ, ppm): Ar–CF_2 −64.0, $-CF_2CF_3$ −81.5, Ar–CF_2 −111.7; MS (*m/z*): 564 (<0.1%) M^+, 545 (2%) $(M - F)^+$, 195 (100%) $(M - C_7F_{15})^+$, 69 (11%) (CF_3). *Elemental analysis*. Calcd. (%) for $C_{15}H_4F_{20}$ (564.2): C 31.93, H 0.71, F 67.35; found: C 31.7, H 0.5, F 67.7.

5.11. 1,8-Bis(4-trifluoromethylphenyl)perfluorooctane (**43**)

The crude product (3.15 g, GC: 84%) was recrystallised from isooctane to afford 1.96 g (40%) white nedlees, mp: 111–112°C. GC: 98.1%, ^{1}H NMR (δ, ppm): H (Ar, *o*-CF_3) 7.73, H (Ar, *m*-CF_3) 7.78, ^{19}F NMR (δ, ppm): Ar–CF_3 −63.9, Ar–CF_2 −111.6, MS (*m/z*): 690 (<0.1%) M^+, 671 (2%) $(M - F)^+$, 195 (100%) $(M - (CF_2)_7Ar)^+$, 69 (4%) (CF_3). *Elemental analysis*. Calcd. (%) for $C_{22}H_8F_{22}$ (690.3): F 60.55; found: F 60.6.

5.12. 1-Perfluorooctyl-3,5-bis(trifluoromethyl)benzene (**44**)

Yield: 4.0 g (64%) colourless oil, bp: 120–130°C (bath temperature) at 16 mmHg. GC: 98.1%, ^{1}H NMR (δ, ppm): H (Ar, *o*-R_{f8}) 8.05, H (Ar, *p*-R_{f8}) 8.12, ^{19}F NMR (δ, ppm): Ar–CF_3 −68.0, Ar–CF_2 −111.6, CF_2CF_3 −81.4, MS (*m/z*): 613 (11%) $(M - F)^+$, 263 (100%) $(M - C_7F_{15})^+$, 69 (57%) (CF_3). *Elemental analysis*. Calcd. (%) for $C_{16}H_3F_{23}$ (632.2): C 30.40, H 0.48, F 69.12; found: C 30.2, H 0.4, F 68.9.

5.13. Methyl 3,5-bis(perfluorooctyl)benzoate (**54**)

Under an argon atmosphere to a stirred mixture of methyl 3,5-dibromobenzoate (4.41 g, 15 mmol), copper bronze (5.21 g, 82 mmol) and absolute dimethyl sulfoxide (50 ml) preheated to ca. 125°C perfluorooctyl iodide (19.2 g, 35 mmol) was added at such a rate to keep the reaction temperature below 135°C. Then, the reaction mixture was stirred at 135°C for 30 h. The reaction mixture was extracted with ether ($6\,ml \times 50$) and the combined ether phase washed with saturated potassium iodide solution ($2\,ml \times 50$). The ether phase was dried (Na_2SO_4) and evaporated. The solid residue (12.75 g) thus obtained was suspended in absolute acetone (30 ml) and filtered (ca. 10°C) to give white crystalline product, 11.5 g (79%), mp: 61–62°C/ether–acetone. GC: 99%. FT-IR: (KBr), ν (cm^{-1}): 1742.9 (C=O), ^{1}H NMR (δ, ppm): CH_3 4.00, H (Ar, *o*-CO) 8.50, H (Ar, *p*-CO) 7.99, ^{19}F NMR (δ, ppm): CF_3 −81.5, Ar–CF_2 −111.6. MS (FAB. NOBA, *m/z*): 973 (43%) $(M + H)^+$, 941 (100%) $(M - OCH_3)^+$, 603 (42%) $(M - C_7F_{15})^+$. *Elemental analysis*. Calcd. (%) for $C_{24}H_6F_{34}O_2$ (972.3): C 29.65, H 0.62, F 66.44; found: C 29.5, H 0.8, F 66.1.

5.14. 3,5-Bis(perfluorooctyl)benzyl alcohol (**55**)

A solution of ester **54** (2.00 g, 2.06 mmol) in absolute ether was treated with $LiAlH_4$ (0.20 g, 4.8 mmol) and refluxed for 5 h. Hydrochloric acid (2 N, 50 ml) was then added and the mixture refluxed for 1 h. The ether phase separated at room temperature and the aqueous phase extracted with ether ($3\,ml \times 30$). The combined ether phase was dried (Na_2SO_4) and evaporated to give 2.0 g of crude product. Recrystallised from dried acetone (ca. 15 ml) and filtered at −10°C. White crystalline product (1.74 g, 90%) was obtained, mp: 101–102°C. GC: 98.6%. FT-IR: (KBr), ν (cm^{-1}): 3427.3 (OH), ^{1}H NMR (δ, ppm): CH_2 4.89, H (Ar, *o*-CH_2) 7.84, H (Ar, *p*-CH_2) 7.74, ^{19}F NMR (δ, ppm): CF_3 −81.4, Ar–CF_2 −111.5. MS (FAB. NOBA, *m/z*): 943 (12%) $(M - H)^+$, 927 (76%) $(M - OH)^+$, 575 (21%) $(M - C_7F_{15})^+$. *Elemental analysis*. Calcd. (%) for $C_{23}H_6F_{34}O$ (944.2): C 29.26, H 0.64, F 68.41; found C 28.9, H 0.8, F 68.1.

5.15. 3.5-Bis(perfluorooctyl)benzaldehyde (**56**)

A solution of alcohol **55** (100 mg, 0.106 mmol) in CH_2Cl_2 (20 ml) was mixed with pyridinium chlorochromate (50 mg, 0.23 mmol) and stirred at room temperature for 24 h. The mixture was then filtered through a Florisil plug (1.5 g) and washed with an additional portion of CH_2Cl_2 (20 ml).

Evaporation gave 85 mg (85%) white crystalline product, mp: 73–74°C. GC: 98.4%, FT-IR: (KBr), ν (cm^{-1}): 1709.7 (C=O), ^{1}H NMR (δ, ppm): CH=O 10.15, H (Ar, *o*-CH=O) 8.33, H (Ar, *p*-CH=O) 8.06, ^{19}F NMR (δ, ppm): CF_3 −81.4, Ar–CF_2 −111.6. MS (FAB. NOBA, *m/z*): 943 (45%) $(M+H)^+$, 941 (100%) $(M-H)^+$, 573 (31%) $(M-C_7F_{15})^+$. *Elemental analysis*. Calcd. (%) for $C_{23}H_4F_{34}O$ (942.2): C 29.32, H 0.43, F 68.55; found: C 29.1, H 0.6, F 68.7.

6. Conclusions

1. Neural network analysis can identify important factors describing fluorophilicity.
2. Traditional QSAR descriptors show a strong non-linearity in describing fluorophilicity, and
3. the use of calculated Hildebrand parameters serves as a first method for the rough estimation of fluorophilicities.

Acknowledgements

This work was supported by the Hungarian Scientific Research Foundation (OTKA, Grant No. T 022169). The COST Action D12 "*Fluorous medium: a tool for environmentally compatible oxidation processes*" is gratefully acknowledged. The authors thank Dr. W. Leitner, Max-Planck-Institute für Kohlenforschung, Mülheim an der Ruhr, for providing samples of (*F*-alkylethyl) arenes; and Ms. Eszter K. Borbás, Eötvös University, Budapest, for her careful technical assistance.

References

[1] D.P. Curran, Chemtracts: Org. Chem. 9 (1996) 75.
[2] B. Cornils, Angew. Chem. Int. Ed. Engl. 36 (1997) 2057.
[3] D.P. Curran, Angew. Chem. Int. Ed. Engl. 37 (1998) 1174.
[4] I.T. Horváth, Acc. Chem. Res. 31 (1998) 641.
[5] E. de Wolf, G. van Koten, B.-J. Deelman, Chem. Soc. Rev. 28 (1999) 37.
[6] R.D. Fish, Chem. Eur. J. 5 (1999) 1677.
[7] M. Cavazzini, F. Montanari, G. Pozzi, S. Quici, J. Fluorine Chem. 94 (1999) 183.
[8] L.P. Barthel-Rosa, J.A. Gladysz, Coord. Chem. Rev. 190-192 (1999) 587.
[9] E.G. Hope, A.M. Stuart, J. Fluorine Chem. 100 (1999) 75.
[10] I.T. Horváth, J. Rábai, Science 266 (1994) 72, and references therein.
[11] I.T. Horváth, J. Rábai, (Exxon Research and Engineering Co.), Chem. Abstr. 123 (1995) 87349; US 5,463,082 (1995).
[12] J.A. Gladysz, Science 266 (1994) 55.
[13] I.T. Horváth, G. Kiss, R.A. Cook, J.E. Bond, P.A. Stevens, J. Rábai, E.J. Mozeleski, J. Am. Chem. Soc. 120 (1998) 3133.
[14] M. Vogt, Ph.D. Thesis, RWTH Aachen, Germany, 1991.
[15] A. Studer, S. Hadida, R. Ferritto, S.-Y. Kim, P. Jeger, P. Wipf, D.P. Curran, Science 275 (1997) 823.
[16] D.P. Curran, S. Hadida, M. Hoshino, A. Studer (University of Pittsburg), Chem. Abstr. 128 (1998) 127604; US 5,777,121 (1998).
[17] D.P. Curran, S. Hadida Ruah, M. Hoshino, A. Studer, P. Wipf, P. Jeger, S.-Y. Kim, R. Ferritto (University of Pittsburg); US 5,859,247 (1999).
[18] A. Studer, D.P. Curran, Tetrahedron 53 (1997) 6681.
[19] A. Studer, P. Jeger, P. Wipf, D.P. Curran, J. Org. Chem. 62 (1997) 2917.
[20] D.P. Curran, S. Hadida, H. Mu, J. Org. Chem. 62 (1997) 6714.
[21] D.P. Curran, R. Ferritto, Y. Hua, Tetrahedron Lett. 39 (1998) 4937.
[22] S. Kainz, Z. Luo, D.P. Curran, W. Leitner, Synthesis (1998) 1425.
[23] R.D. Chambers, C. Magron, G. Sanford, J. Chem. Soc., Perkin Trans. 1 (1999) 283.
[24] I.T. Horváth, in: B. Cornils, W.A. Herrmann (Eds.), Applied Homogeneous Catalysis with Organometallic Compounds, Vols. 1 and 2, VHC, Weinheim, 1996, pp. 601–605.
[25] G. Pozzi, M. Cavazzini, F. Cinato, F. Montanari, S. Quici, Eur. J. Org. Chem. (1999) 1947.
[26] Y. Nakamura, S. Takeuchi, Y. Ohgo, D.P. Curran, Tetrahedron 56 (2000) 351.
[27] P. Wipf, J.T. Reeves, Tetrahedron Lett. 40 (1999) 4649.
[28] I. Ryu, T. Niguma, S. Minakata, M. Komatsu, Z. Luo, D.P. Curran, Tetrahedron Lett. 40 (1999) 2367–2370.
[29] S. Röver, P. Wipf, Tetrahedron Lett. 40 (1999) 5667.
[30] D.P. Curran, Z. Luo, J. Am. Chem. Soc. 121 (1999) 9069.
[31] J.C. Giddings, Unified Separation Science, Wiley, New York, 1991, pp. 16–36.
[32] A.F.M. Barton, Chem. Rev. 75 (1975) 731.
[33] A.F.M. Barton, CRC Handbook of Solubility Parameters and Other Cohesion Parameters, CRC Press, Boca Raton, FL, 1983.
[34] J.H. Hildebrand, R.L. Scott, The Solubility of Nonelectrolytes, 3rd Edition, Dover, New York, 1964.
[35] P.A. Small, J. Appl. Chem. 3 (1953) 71.
[36] C. Hansch, Acc. Chem. Res. 2 (1969) 232.
[37] M.J. Kamlet, R.M. Doherty, M.H. Abraham, R.A. Taft, Quant. Struct.-Act. Relat. 7 (1988) 71.
[38] D.B. Smithrud, F. Diederich, J. Am. Chem. Soc. 112 (1990) 339.
[39] R.T. Baker, W. Tumas, Science 284 (1999) 1477.
[40] R. Fink, D. Hancu, R. Valentine, E.J. Beckman, J. Phys. Chem. B 103 (1999) 6441.
[41] T. Sarbu, T. Styranec, E.J. Beckman, Nature 405 (2000) 165.
[42] W. Chen, L. Lu, J. Xiao, Org. Lett. 2 (2000) 2675.
[43] D. Koch, W. Leitner, J. Am. Chem. Soc. 120 (1998) 13398.
[44] L. Solé-Violan, B. Devallez, M. Postel, J.G. Riess, New J. Chem. 17 (1993) 581.
[45] D.P. Curran, S. Hadida, J. Am. Chem. Soc. 118 (1996) 2531.
[46] D.P. Curran, M. Hoshino, J. Org. Chem. 61 (1996) 6480.
[47] R.P. Hughes, H.A. Trujillo, Organometallics 15 (1996) 286.
[48] V. Herrera, P.J.F. de Rege, I.T. Horváth, T.L. Husebo, R.P. Hughes, Inorg. Chem. Commun. 1 (1998) 197.
[49] L.J. Alvey, D. Rutherford, J.J.J. Juliette, J.A. Gladysz, J. Org. Chem. 63 (1998) 6302.
[50] L.E. Kiss, J. Rábai, L. Varga, I. Kövesdi, Synlett (1998) 1243.
[51] Z. Szlávik, G. Tárkányi, Gy. Tarczay, Á. Gömöry, J. Rábai, J. Fluorine Chem. 98 (1999) 83.
[52] S. Quici, M. Cavazzini, S. Ceragioli, F. Montanari, G. Pozzi, Terahedron Lett. 40 (1999) 3647.
[53] A. Klose, J.A. Gladysz, Tetrahedron: Asymmetry 10 (1999) 2665.
[54] J.J.J. Juliette, D. Rutherford, I.T. Horváth, J.A. Gladysz, J. Am. Chem. Soc. 121 (1999) 2696.
[55] B. Linclau, A.K. Singh, D.P. Curran, J. Org. Chem. 64 (1999) 2835.
[56] D.P. Curran, S. Hadida, S.-Y. Kim, Z. Luo, J. Am. Chem. Soc. 121 (1999) 6607.
[57] B. Betzemeier, F. Lhermitte, P. Knochel, Synlett (1999) 489.
[58] B. Richter, B.-J. Deelman, G. van Koten, J. Mol. Catal. A 145 (1999) 317.
[59] C.H. Winter, X.-X. Zhou, in: J.S. Thrasher, S.H. Strauss (Eds.), Inorganic Fluorine Chemistry Toward the 21st Century, Proceedings of the ACS Symposium Series 555, American Chemical Society, Washington, DC, 1994, pp. 366–382.

[60] Z. Szlávik, G. Tárkányi, Á. Gömöry, G. Tarczay, J. Rábai, J. Fluorine Chem., in press.
[61] B. Richter, A.L. Spek, G. van Koten, B.-J. Deelman, J. Am. Chem. Soc. 122 (2000) 3945.
[62] B. Richter, E. deWolf, G. van Koten, B.-J. Deelman, J. Org. Chem. 65 (2000) 3885.
[63] http://www.organik.uni-erlangen.de/gladysz/research/partition.html.
[64] A.J. Leo, Chem. Rev. 93 (1993) 1281.
[65] M.H. Abraham, Quantitative Treatments of Solute/Solvent Interactions, Elsevier, New York, 1994.
[66] HyperChem, version 4.0, HyperCube Inc., Canada, 1997.
[67] IsisBase version 1.2 for desktop, Molecular Design Ltd., 1996.
[68] 3DNET version 1.0, CompElite Ltd., Hungary, 1998.
[69] I. Kövesdi, M.F. Dominquez-Rodriquez, L. Örfi, G. Náray-Szabó, A. Varró, J.Gy. Papp, P. Mátyus, Med. Res. Rev. 19 (1999) 249.
[70] M.L. Connolly, J. Am. Chem. Soc. 107 (1985) 1118.
[71] A.Y. Meyer, J. Chem. Soc. Rev. 15 (1986) 449.
[72] R. Todeschini, P. Gramatica, Quant. Struct.-Act. Relat. 16 (1997) 120.
[73] K. Iwase, K. Komatau, S. Hirono, S. Nakagawa, I. Moriguchi, Chem. Pharm. Bull. 33 (1985) 2114.
[74] J. De Bruijn, J. Hermens, J. Quant. Struct-Act. Relat. 9 (1990) 11.
[75] A. Breindl, B. Beck, T. Clark, R.C. Glen, J. Mol. Model. 3 (1997) 142.
[76] K.J. Miller, J. Am. Chem. Soc. 112 (1990) 8533.
[77] W.J. Mortier, K. van Genechten, J. Gasteiger, J. Am. Chem. Soc. 107 (1985) 829.
[78] P. Broto, G. Moreau, C. Vandycke, Eur. J. Med. Chem. 19 (1984) 71.
[79] R.F. Fedors, D.W. Van Krevelen, P.J. Hoftyzer, in: A.F.M. Barton, CRC Handbook of Solubility Parameters and Other Cohesion Parameters, CRC Press, Boca Raton, FL, 1983, pp. 64–66.
[80] P.R. Andrews, D.J. Craik, J.L. Martin, J. Med. Chem. 27 (1984) 1648.
[81] H. Wiener, J. Am. Chem. Soc. 69 (1947) 2636.
[82] M. Randic, J. Am. Chem. Soc. 97 (1975) 6609.
[83] A.R. Katritzky, V.S. Lobanov, M. Karelson, J. Chem. Inf. Comput. Sci. 38 (1988) 28.
[84] N. Bodor, M.J. Huang, A. Harget, J. Mol. Struct. (Theochem) 309 (1994) 259.
[85] P. Gaillard, P. Carrupt, B. Testa, A. Boudon, J. Comput.-Aided Mol. Des. 8 (1994) 83.
[86] T.D. Cronce, G.R. Famini, J.A. De Soto, L.Y. Wilson, J. Chem. Soc., Perkin Trans. 2 (1998) 1293.
[87] N. Bodor, P. Buchwald, J. Phys. Chem. B 101 (1997) 3404.
[88] Kröse, P. van der Smagt, An Introduction to Neural Networks, 1997. http://www.fwi.uva.nl/research/neuro.
[89] T. Masters, Practical Neural Network Recipes in C++, Academic Press, Boston, 1996.
[90] X.H. Yu, IEEE Trans. Neur. Net. 3 (1992) 1019.
[91] K. Hornik, M. Stinchcombe, H. White, J. Neur. Net. 5 (1989) 359.
[92] E. Hartman, J.D. Keeler, J.M. Kowalski, Neur. Comput. 2 (1990) 210.
[93] K. Hornik, M. Stinchcombe, H. White, P. Auer, Neur. Net. 5 (1994) 1262.
[94] B.L. Kalman, S.C. Kwasny, Proceedings of the International Conference on Neural Networks, Baltimore, 1992.
[95] F. Despagne, L. Massart, Chemom. Intell. Lab. Syst. 40 (1996) 145.
[96] F.O. Andersson, M. Aberg, S.P. Jacobson, Chemom. Intell. Lab. Syst. 51 (2000) 61.
[97] J. Zupan, J. Gasteiger, Neural Networks for Chemists, VCH, Weinheim, 1993.
[98] N.R. Draper, H. Smith, Applied Regression Analysis, Wiley, New York, 1981.
[99] L.E. Kiss, I. Kövesdi, J. Rábai, Proceedings of the 16th International Symposium on Fluorine Chemistry, Durham, UK, July 2000, Abstract, C-23.
[100] P. Camilleri, S. Watts, J. Boratson, J. Chem. Soc., Perkin Trans. 2 (1988) 1699.
[101] W.S. Friedlander (to 3M Co.) US 3,088,849 (1961); Chem. Abstr. 59 (1963) 11258b.
[102] C. Wakselman, M. Tordeaux, J. Org. Chem. 50 (1985) 4047.
[103] A.E. Feiring, J. Fluorine Chem. 24 (1984) 191.
[104] A. Dasgupta, P.E. Humphrey, J. Chromatogr. B 708 (1998) 299.
[105] C. Kimura, K. Kashiwaya, M. Kobayashi, T. Nishiyama, J. Am. Oil Chem. Soc. 69 (1984) 105.
[106] K.J.L. Paciorek, R.H. Kratzer, H.M. Atkins, J. Fluorine Chem. 53 (1991) 365.
[107] A.B. Cowell, C. Tamborski, J. Fluorine Chem. 17 (1981) 345.
[108] A. Schulte, V.M. Hollmark, R. Twieg, K. Song, J.F. Rabolt, Macromolecules 24 (1991) 3901.
[109] S. Kainz, D. Koch, W. Baumann, W. Leitner, Angew. Chem. Int. Ed. Engl. 36 (1997) 1628.
[110] S. Kainz, D. Koch, W. Baumann, W. Leitner, Angew. Chem. 109 (1997) 1699.
[111] S. Kainz, Z. Luo, D.P. Curran, W. Leitner, Synthesis (1998) 1425.
[112] T. Umemoto, Y. Kuriu, H. Shuyama, Chem. Lett. (1981) 1663.
[113] G. Pozzi, I. Colombani, M. Miglioli, F. Montanari, S. Quici, Tetrahedron 53 (1997) 6145.
[114] G. Pozzi, F. Montanari, S. Quici, J. Chem. Soc., Chem. Commun. (1997) 69.
[115] B.-N. Huang, J.-T. Liu, J. Fluorine Chem. 64 (1993) 37.
[116] B. Huang, J. Liu, Tetrahedron Lett. 31 (1990) 2711.